

Summary: This manuscript presents an interesting study of aerosol nitrate formation in an elevated urban environment (Lhasa, Tibetan Plateau, China), with a focus on stable triple oxygen isotope measurements of aerosol nitrate. The authors collected high-volume aerosol samples for offline chemical and isotopic analyses and used the oxygen isotopic composition of nitrate ($\Delta^{17}\text{O}$) to infer the seasonality, and to a limited extent, diurnal variation of NO_x oxidation and nitrate formation pathways. They conclude that oxidation by $\text{NO}_3 + \text{VOC}$ contributes significantly to aerosol nitrate formation (~26%) based on a Bayesian isotope mixing model. While this study is timely and potentially impactful, particularly due to the high-elevation urban setting and the application of oxygen isotopes, it suffers from major methodological limitations and interpretive leaps. For example, the mixing model appears to be significantly underconstrained, and key assumptions (e.g., endmember $\Delta^{17}\text{O}$ values) are not adequately justified or tested. The manuscript would benefit from deeper contextualization, more rigorous uncertainty analysis, and supplemental modeling to support the stated conclusions. I believe the study has potential but requires substantial revision before it can be considered for publication in ACP.

Response: Thanks for your valuable comments, which really helped improve the manuscript. Below, we will provide a detailed and point-by-point response to your comments. All the changes have been included in the latest manuscript (Reviewers' and Editorial Office's comments are in italics; our responses are in regular font).

Comments:

1. Text S2: This section is never referenced in the main manuscript but contains a critical assumption about the fraction of NO_2 oxidation. Since the $\Delta^{17}\text{O}(\text{NO}_3^-)$ signature is largely derived from NO_2 , this section should be moved to the main text.

Response: Thanks for your suggestion. We have moved Text S2 to Section 2.4. **(Line 150-191)**

Line 150-191: 2.4 Evaluation of NO_3^- oxidation pathways

In our study, we aimed to quantify the relative contribution of different oxidation pathways to NO_3^- production based on $\Delta^{17}\text{O}-\text{NO}_3^-$. Due to the low Cl^- concentrations observed in Lhasa, the NO_3^- formation pathways considered in this study are limited to NO_2+OH , NO_3+VOC , and $\text{N}_2\text{O}_5+\text{H}_2\text{O}$. Although NO_3+VOC is generally considered a minor pathway in continental regions (Alexander et al., 2009), we included it because elevated VOC concentrations were observed at our sampling site in Lhasa, influenced by both biogenic emissions (e.g. incense burning) and anthropogenic sources (e.g. vehicle emissions) (Tang et al., 2022). The relative contributions of the three pathways were determined using a $\Delta^{17}\text{O}$ -based mass balance approach (Michalski et al., 2003), as shown in Equations (1) and (2):

$$\Delta^{17}\text{O}-\text{NO}_3^- = (\Delta^{17}\text{O}-\text{NO}_3^-)_{\text{NO}_2+\text{OH}} \times f_{\text{NO}_2+\text{OH}} + (\Delta^{17}\text{O}-\text{NO}_3^-)_{\text{NO}_3+\text{VOC}} \times f_{\text{NO}_3+\text{VOC}} + (\Delta^{17}\text{O}-\text{NO}_3^-)_{\text{N}_2\text{O}_5+\text{H}_2\text{O}} \times f_{\text{N}_2\text{O}_5+\text{H}_2\text{O}} \quad (1)$$

$$f_{\text{NO}_2+\text{OH}} + f_{\text{NO}_3+\text{VOC}} + f_{\text{N}_2\text{O}_5+\text{H}_2\text{O}} = 1 \quad (2)$$

where $\Delta^{17}\text{O}-\text{NO}_3^-$ value is the $\Delta^{17}\text{O}$ value of NO_3^- in $\text{PM}_{2.5}$. The $(\Delta^{17}\text{O}-\text{NO}_3^-)_{\text{NO}_2+\text{OH}}$, $(\Delta^{17}\text{O}-\text{NO}_3^-)_{\text{NO}_3+\text{VOC}}$, and $(\Delta^{17}\text{O}-\text{NO}_3^-)_{\text{N}_2\text{O}_5+\text{H}_2\text{O}}$ correspond to the $\Delta^{17}\text{O}$ values from $\text{NO}_2 + \text{OH}$, $\text{NO}_3 + \text{VOC}$ and $\text{N}_2\text{O}_5 + \text{H}_2\text{O}$, respectively. The $\Delta^{17}\text{O}$ values for each pathway were calculated using Equations (3), (4), and (5) (Savarino et al., 2016; Alexander et al., 2009):

$$(\Delta^{17}\text{O}-\text{NO}_3^-)_{\text{NO}_2+\text{OH}} (\text{‰}) = 2/3\alpha \times \Delta^{17}\text{O}-\text{O}_3^* \quad (3)$$

$$(\Delta^{17}\text{O}-\text{NO}_3^-)_{\text{NO}_3+\text{VOC}} (\text{‰}) = 2/3\alpha \times \Delta^{17}\text{O}-\text{O}_3^* + 1/3 \times \Delta^{17}\text{O}-\text{O}_3^* \quad (4)$$

$$(\Delta^{17}\text{O}-\text{NO}_3^-)_{\text{N}_2\text{O}_5+\text{H}_2\text{O}} (\text{‰}) = 1/3\alpha \times \Delta^{17}\text{O}-\text{O}_3^* + 1/2(2/3\alpha \times \Delta^{17}\text{O}-\text{O}_3^* + 1/3 \times \Delta^{17}\text{O}-\text{O}_3^*) \quad (5)$$

Previous studies have demonstrated a linear correlation between $\Delta^{17}\text{O}-\text{O}_3$ and $\Delta^{17}\text{O}-\text{O}_3^*$, with $\Delta^{17}\text{O}(\text{O}_3)$ values ranging from 20% to 40% in tropospheric O_3 (Vicars and Savarino, 2014; Ishino et al., 2017). The equations are shown as follows (Vicars et al., 2012):

$$\Delta^{17}\text{O}-\text{O}_3^* = 1.5 \times \Delta^{17}\text{O}-\text{O}_3 \quad (6)$$

Based on previous observations of tropospheric O_3 , $\Delta^{17}\text{O}-\text{O}_3^*$ average value was approximately 39‰. The α value represents the proportional contribution of O_3 to the NO oxidation pathway and can be estimated using the following equations (7)

(Alexander et al., 2009). When NO_x is in photochemical steady state, $\Delta^{17}\text{O-NO}_2$ can be represented using the following equation (10):

$$\alpha = K_{P1} [\text{O}_3] \times [\text{NO}] / (K_{P1} \times [\text{O}_3] \times [\text{NO}] + K_{P2} \times [\text{NO}] \times [\text{HO}_2] + K_{P3} \times [\text{NO}] \times [\text{RO}_2]) \quad (7)$$

$$K_{P1} = 3.0 \times 10^{-12} \times e^{(-1500/T)} \quad (8)$$

$$K_{P2} = K_{P3} = 3.5 \times 10^{-12} \times e^{(270/T)} (\text{cm}^3 \cdot \text{molecule}^{-1} \cdot \text{s}^{-1}) \quad (9)$$

$$\Delta^{17}\text{O-NO}_2 = \alpha \Delta^{17}\text{O-O}_3^* \quad (10)$$

where T represents the ambient temperature (K) (Kunasek et al., 2008). The HO₂ mixing ratios were estimated using empirical equations in the absence of direct HO₂ observations (Kanaya et al., 2007). Due to the lower temperatures in Lhasa during non-summer seasons, HO₂ concentrations were assessed using a formula derived from winter conditions.

Winter

$$[\text{HO}_2 \cdot] / \text{ppt} = \exp (5.7747 \times 10^{-2} [\text{O}_3] (\text{ppb}) - 1.7227) \text{ for daytime} \quad (11)$$

$$[\text{HO}_2 \cdot] / \text{ppt} = \exp (7.7234 \times 10^{-2} [\text{O}_3] (\text{ppb}) - 1.6363) \text{ for nighttime} \quad (12)$$

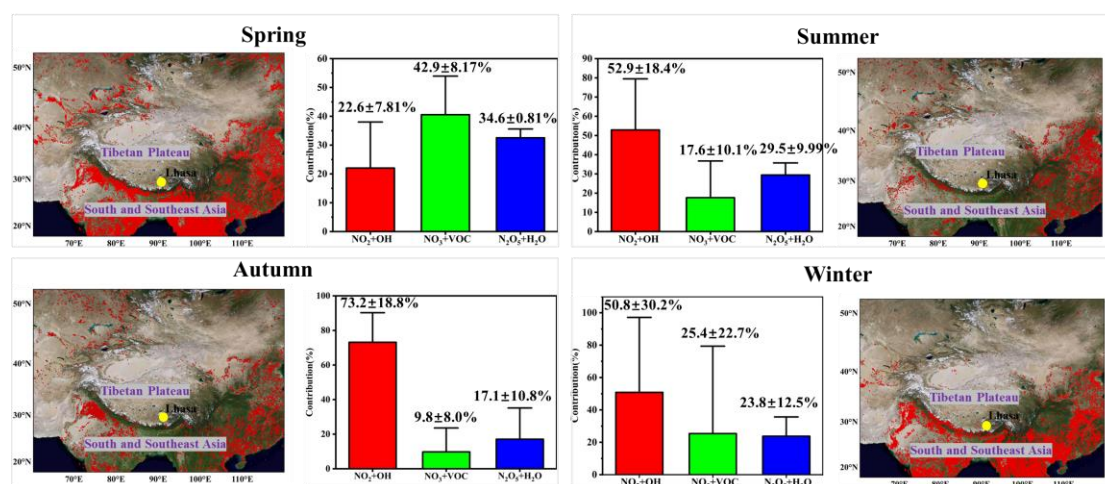
Summer

$$[\text{HO}_2 \cdot] / \text{pptv} = \exp (2.0706 \times 10^{-2} [\text{O}_3] (\text{ppb}) + 1.0625) \text{ for daytime} \quad (13)$$

$$[\text{HO}_2 \cdot] / \text{pptv} = 0.2456 + 0.1841 [\text{O}_3] (\text{ppb}) \text{ for nighttime} \quad (14)$$

2. TOC Figure: *The figure may mislead readers by implying significant seasonal differences in $\Delta^{17}\text{O}(\text{NO}_3^-)$ that are not statistically supported in the results. Differences were observed only in spring. Uncertainties must be included for the pathway contributions, and once added, the seasonal distinctions may not hold.*

Response: Thanks for your suggestion. We have revised the TOC figure to more accurately reflect the findings in the revised manuscript.



3. Lines 35–37: The uncertainty in the calculated pathway contributions should be provided.

Response: Thanks for your valuable suggestion. We have added it to the revised manuscript. (Line 42-44)

Line 42-44: Our results show that NO₂ + OH is the largest contributor to NO₃⁻ formation (46 ± 26%), followed by NO₃ + VOC (26 ± 18%), and N₂O₅ + H₂O (28 ± 11%) using the Bayesian Isotope Mixture Model.

4. Lines 37–39: Explain how this difference between seasons was determined

Response: Thanks for your suggestion. We have added it to the revised manuscript. (Line 44-45)

Line 44-45: Notably, there are significant differences in the NO₂ + OH, NO₃ + VOC, and N₂O₅ + H₂O pathways between spring and other three seasons (T test, $p < 0.05$).

5. Lines 39–40: Add context to how these statements were concluded.

Response: Thanks for your suggestion. We have added it to the revised manuscript. (Line 47-50)

Line 47-50: By Hybrid Single-Particle Lagrangian Integrated Trajectory (HYSPLIT) dispersion model, we highlighted the influence of VOC emissions from regions such as Afghanistan and northern India, which enhanced NO₃⁻ concentrations in Lhasa during spring.

6. Line 42: *Acronyms such as ALWC, NO₃⁻, and VOC are not defined in the abstract and should be introduced.*

Response: Thanks for your suggestion, we have added all acronyms to the revised manuscript. **(Line 39-41/Line 50-53)**

Line 39-41: Atmospheric particulate nitrate aerosol (NO₃⁻), produced via the oxidation of nitrogen oxides (NO_x = NO + NO₂), plays an important role in atmospheric chemistry and air quality, yet its formation mechanism remains poorly constrained in the plateau region.

Line 50-53: Furthermore, the diurnal distribution of NO₃⁻ oxidation pathways varied distinctly across seasons, suggesting that these differences in NO₃⁻ pathways are attributed to aerosol liquid water content (ALWC), volatile organic compounds (VOC) concentration, and pollution levels.

7. Lines 87–89: *It is unusual to target three "major" NO₃⁻ formation pathways in a continental setting, especially including NO₃ + VOC, which is generally minor. Consider referencing Alexander et al., 2019 and revisiting the classification of major pathways.*

Response: Thanks for your suggestion. (1) We acknowledge that in many continental environments, NO₃ + VOC pathway is generally considered a minor contributor to NO₃⁻ formation. However, recent observation-based studies have increasingly reported that this pathway can play a significant role in NO₃⁻ production under certain atmospheric conditions (Zhang et al., 2022; Fan et al., 2021; Feng et al., 2023; Li et al., 2022).

(2) Our sampling site is located in the central urban area of Lhasa, where air masses are influenced by both biogenic and anthropogenic sources of Volatile Organic Compounds (VOC), including biomass burning and incense burning. Tang et al. (2022) have shown that VOC concentrations in Lhasa are comparable to those in the North China Plain, supporting the plausibility of a significant contribution from the NO₃ + VOC pathway in this region.

(3) To address the reviewer's concern, we have now cited the perspective provided by

Alexander et al. (2009) in the revised manuscript. We have also clarified that the classification of the major pathways in this study is based on region-specific observational evidence, rather than general assumptions **(Line 156-159)**.

Line 156-159: Although $\text{NO}_3 + \text{VOC}$ was generally considered a minor pathway in continental regions (Alexander et al., 2009), we included it because elevated VOC concentrations were observed at our sampling site in Lhasa, influenced by both biogenic emissions (e.g. incense burning) and anthropogenic sources (e.g. vehicle emissions) (Tang et al., 2022).

8. Lines 93–94: *Since the site is at high elevation, provide information on altitude-related meteorology and its influence on boundary layer mixing and transport.*

Response: Thanks for your suggestion. We have added it to the revised manuscript. **(Line 111-114)**

Line 111-114: The strong solar radiation and large diurnal temperature variations in this sampling site can lead to pronounced changes in boundary layer height, which in turn significantly influence vertical mixing and the transport of air pollutants.

9. Lines 94–95: *Include more detail on the urban characteristics and land use of Lhasa to contextualize emissions.*

Response: Thanks for your suggestion. We have added it to the revised manuscript. **(Line 107-111)**

Line 107-111: $\text{PM}_{2.5}$ samples were collected on the roof of a building (~15 m above ground) at the Meteorological Bureau of Lhasa (91.08°E, 29.40°N; Figure 1) in China. Lhasa, the capital of the Tibet Autonomous Region, is a rapidly developing city with a population of ~ 950000 and an urban area of ~ 30000 km^2 (Lhasa). The sampling site is surrounded by mixed land use, including residential areas, government offices, religious temples and commercial zones, with minimal heavy industry.

10. Lines 125–126: *The link did not work. Ensure that all supplemental data used in the manuscript is archived and accessible via a reliable digital repository.*

Response: Thanks for checking carefully. The link has been updated in our revised manuscript. **(Line 149-151)**

Line 149-151: Additionally, NO₂ and O₃ during the sampling campaign were downloaded from the National Meteorological Information Center (<https://air.cnemc.cn:18007/>).

11. Lines 131–132: *The isotope mixing model assumes known $\Delta^{17}\text{O}$ endmembers. How were these determined, particularly for $\Delta^{17}\text{O}(\text{NO}_2)$? Please explain the derivation or source of these values.*

Response: Thank you for your suggestion. We have added detailed explanation of the derivation of $\Delta^{17}\text{O}$ endmember values, particularly for $\Delta^{17}\text{O}(\text{NO}_2)$, in Section 2.4 of the revised manuscript.

12. Lines 150–153: *The MDL for NO₃⁻ was given earlier (Line 114), but MDLs for other ions are missing here. Please include them.*

Response: Thanks for your comment. We have now included MDLs for other relevant ions in the revised manuscript. **(Line 136-138)**

Line 136-138: The method detection limits (MDLs) for Cl⁻, NO₃⁻, SO₄²⁻, Na⁺, NH₄⁺, K⁺, Mg²⁺, and Ca²⁺ were 0.001 mg/L, 0.001 mg/L, 0.003 mg/L, 0.02 mg/L, 0.01 mg/L, 0.02 mg/L, 0.006 mg/L, and 0.02 mg/L, respectively.

13. Lines 154–157: *The provided URL for the model is not a proper citation. Please cite the model formally and ensure access.*

Response: Thanks for checking carefully. We have replaced the proper URL in the manuscript. **(Line 225)**

Line 225: <https://www.ready.noaa.gov/HYSPLIT>.

14. Lines 157–159: *Add a supporting reference for the assumptions or parameterizations described here.*

Response: Thanks for your suggestion. We have added supporting references in the

manuscript. **(Line 225-227)**

Line 225-227: This model has been widely used for simulating the transport and dispersion trajectories of pollutants such as PM_{2.5}, VOC, O₃, and NO_x, among others (He et al., 2022; Zhao et al., 2015; Cao et al., 2023).

15. Lines 159–162: Why was 3,650 meters chosen for the model?

Response: Thanks for your comment. The height of 3650 meters was chosen because it corresponds to the actual altitude of our sampling site in Lhasa. To ensure consistency between the modeled air mass trajectories and the observational data, we used the same elevation as the receptor height in the HYSPLIT simulations.

16. Lines 173–175: The claim of an "opposite" trend is unclear; visually, it seems the trends are actually consistent. Please clarify.

Response: Thank you very much for your careful review and insightful comment. We agree that the original expression “opposite trend” was inaccurate and could cause confusion. We have revised it in the revised manuscript. **(Line 241-243)**

Line 241-243: Solar radiation intensity exhibited a seasonal trend consistent to those of temperature and RH, peaking in summer (394 W/m²) and reaching its lowest levels in winter (220 W/m²).

17. Lines 179–200: Nitrate concentrations depend strongly on gas-particle partitioning, which is influenced by chemical composition (e.g., NH₄⁺) and meteorology. Discuss the observed spring peak in NO₃⁻ alongside NH₄⁺ trends and partitioning behavior of HNO₃.

Response: Thanks for your valuable comment. Although we did not measure gaseous HNO₃ in this study, we conducted correlation analysis between NO₃⁻ and NH₄⁺, Ca²⁺, and K⁺ concentrations, as well as temperature and relative humidity. We acknowledge the absence of HNO₃ data limits a full assessment of partitioning behavior. We will address this aspect more comprehensively in future studies using online gas-phase measurements and thermodynamic modelling **(Line 252-258).**

Line 252-258: NO_3^- mass concentrations ranged from 0.10 to 1.72 $\mu\text{g}/\text{m}^3$, with an average value of $0.62 \pm 0.31 \mu\text{g}/\text{m}^3$. NO_3^- concentrations exhibited distinct seasonal patterns. As shown in Figure S1, the equivalent concentrations of $[\text{SO}_4^{2-} + \text{NO}_3^-]$ were considerably higher than those of $[\text{NH}_4^+]$, indicating that NH_4^+ was insufficient to fully neutralize NO_3^- . This suggests that a portion of NO_3^- may have existed in other forms, such as KNO_3 and $\text{Ca}(\text{NO}_3)_2$. This inference is supported by the strong positive correlations between NO_3^- and K^+ ($r = 0.64$, $p < 0.1$) and Ca^{2+} ($r = 0.43$, $p < 0.01$), especially in spring, as shown in Figure S2. In contrast, NO_3^- showed relatively weak negative correlations with T ($r = -0.27$, $p < 0.01$) and RH ($r = -0.22$, $p < 0.1$), indicating that under the specific atmospheric conditions in Lhasa, meteorological parameters might not be the dominant factors controlling the gas-particle partitioning of NO_3^- . The maximum monthly average values of NO_3^- concentration occurred in spring ($0.83 \pm 0.35 \mu\text{g}/\text{m}^3$) with the instantaneous maximum reaching 1.72 $\mu\text{g}/\text{m}^3$, whereas the lowest was recorded in autumn ($0.23 \pm 0.13 \mu\text{g}/\text{m}^3$) with an instantaneous minimum of only 0.09 $\mu\text{g}/\text{m}^3$ (Table 1). The elevated NO_3^- concentrations in spring could be attributed to biomass burning emitted from south and Southeast Asia (Figure S3/Figure S4). The strong between NO_3^- and K^+ in spring further this explanation.

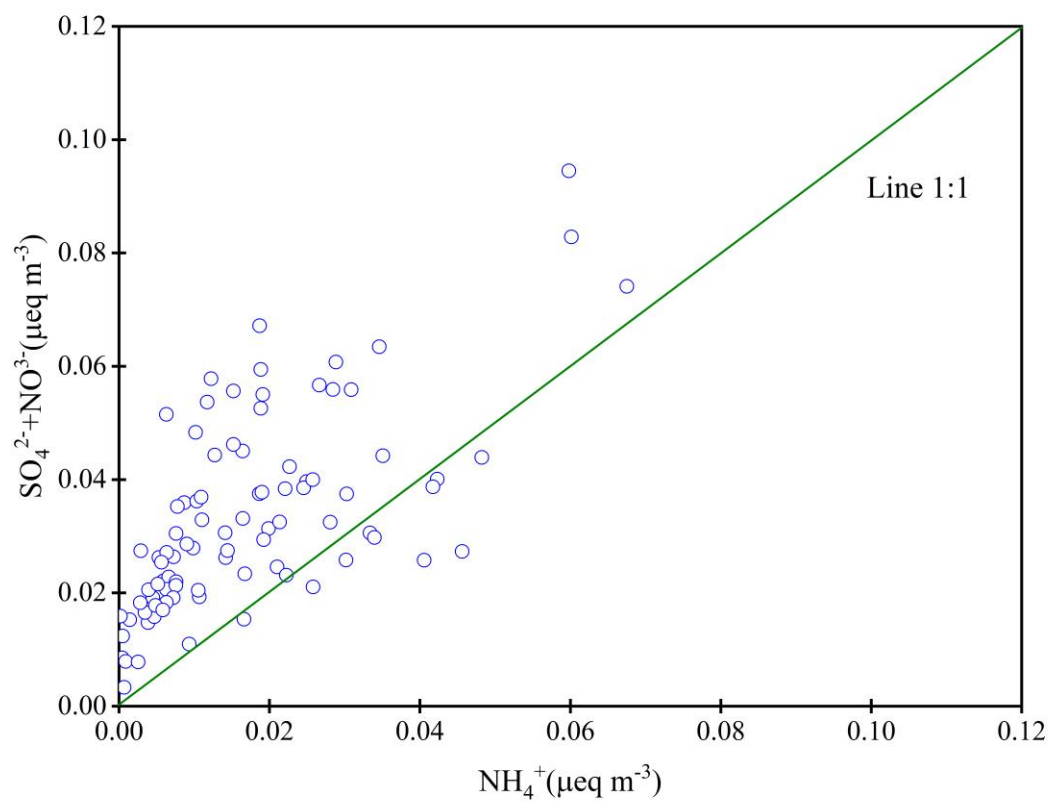


Figure S1 Equivalent concentrations of $\text{SO}_4^{2-} + \text{NO}_3^- / \text{NH}_4^+$ in Lhasa during the sampling campaign.

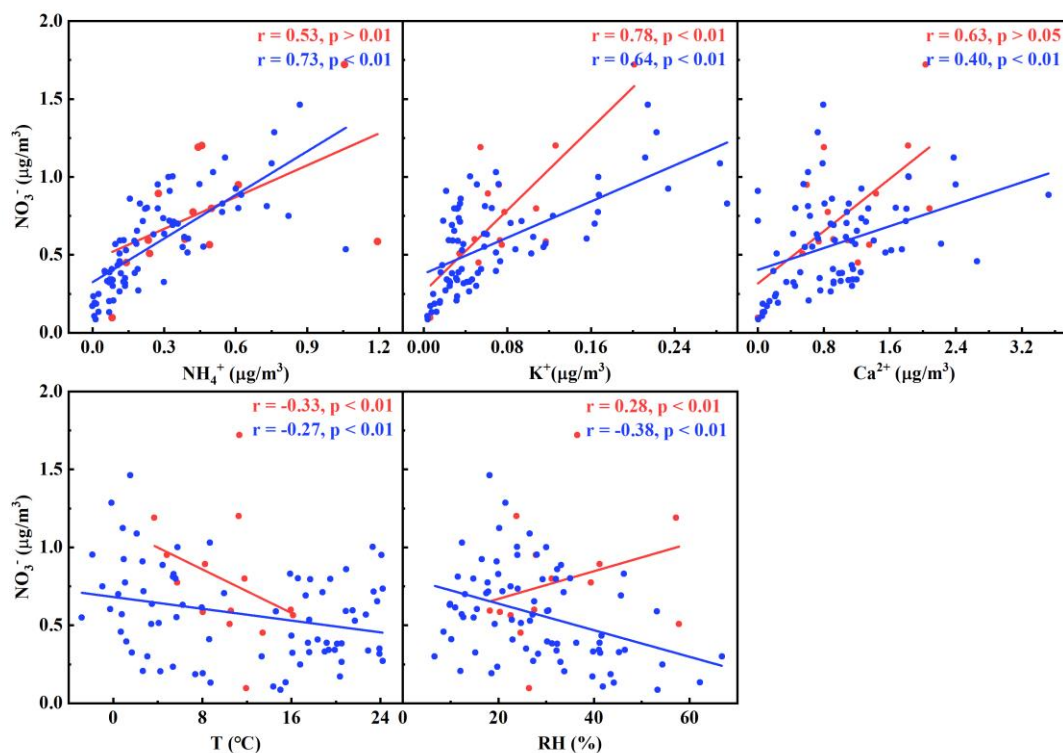


Figure S2 Relationships between NO_3^- and other parameters. The relationship between NO_3^- and (a) NH_4^+ concentrations, (b) K^+ concentrations (c) Ca^{2+} , (d) T , and (e) RH ; The red and blue represent spring and other seasons.

18. Lines 186–188: Provide a possible explanation for the observed concentration increase. Is there a local emission or meteorological reason?

Response: Thanks for your suggestion. We have added a more detailed explanation for the observed springtime NO_3^- concentration increase. Specifically, we suggest that the weak southeasterly winds may have limited atmospheric dispersion, leading to local accumulation of NO_3^- precursors. Furthermore, the southeast sector may be influenced by traffic or agricultural sources, which could contribute to the enhanced NO_3^- production. We have added it to the revised manuscript. (**Line 265-270**)

Line 265-270: The southeasterly sector of sampling site includes residential areas, agriculture land and major transportation routes, which are potential NO_x sources. In spring, intensified agriculture activities (e.g., fertilization, biomass burning) increase emissions. Meanwhile, low wind speeds likely limit atmospheric dispersion, promoting the local accumulation of precursors and enhancing NO_3^- production.

19. Lines 190–191: *The COVID-19 shutdown period seems to have ended before sampling. If not, describe local shutdown policies in the methods section.*

Response: Thanks for your careful and constructive comment. We confirm that part of the sampling period, specifically during autumn 2022, coincided with strict COVID-19 control measures in Lhasa. During this period, the city implemented targeted lockdowns with near-total restrictions on vehicle traffic and pedestrian movement. We have added a description of these local measures in the methods section in the revised manuscript to clarify the context during sampling (**Line 121-123**).

Line 121-123: During the autumn of 2022, Lhasa experienced intermittent COVID-19 control measures, including restricted movement, reduced traffic activity, and temporary lockdowns in urban areas (Daily).

20. Lines 191–195: *This statement implies minimal local influence. Consider emphasizing regional transport instead.*

Response: Thanks for pointing this out. We acknowledge that the original statement may have underemphasized the potential role of regional transport. We have revised the relevant sentences to clarify that although local emissions were suppressed due to COVID-19 lockdowns in autumn, the persistence of detectable NO_3^- concentrations under stagnant conditions suggests a likely contribution from regional transport. We have revised it in the manuscript (**Line 270-284**).

Line 270-284: During the rainy summer, shorter NO_3^- lifetimes indicated a weak influence from regional transport, with a more pronounced contribution from local emissions. In autumn, NO_3^- concentrations were relatively low, which coincided with strict local COVID-19 restrictions in Lhasa. These measures significantly reduced human activity and traffic, leading to suppressed local emissions. Despite low wind speeds typically favor pollutant accumulation, NO_3^- concentrations remained low, suggesting that both reduced local sources and seasonal meteorological conditions constrained NO_3^- production. Nevertheless, the persistence of measurable NO_3^- under such stagnant conditions also implied a potential contribution from regional transport during this period. In winter, elevated NO_3^- concentrations under low wind speeds (< 3

m/s) emphasized the significant contribution of local emissions. These findings underscored that both regional transport and local emissions were important contributors to NO_3^- concentrations in Lhasa.

21. Lines 193–195: *If COVID-19 restrictions impacted emissions, explain why no corresponding impact is evident in your data.*

Response: Thanks for insightful comment. Although local COVID-19 restrictions likely reduced emissions, NO_3^- was still detectable during autumn, possibly due to background levels and regional transport. We have clarified this in the revised text by acknowledging that reduced local emissions alone may not fully explain the observed concentrations, and that regional transport may have contributed to the persistence of NO_3^- .

22. Lines 213–215: *The data do not clearly show seasonal differences. Spring appears elevated, but other seasons are similar. Please clarify the interpretation.*

Response: Thanks for your helpful comment. We agree with your assessment. In the revised manuscript, we have removed the original sentence that inaccurately suggested clear seasonal variation in $\Delta^{17}\text{O}-\text{NO}_3^-$ values. **(Line 298-300:)**

Line 298-300: As shown in Table S2, the observed $\Delta^{17}\text{O}-\text{NO}_3^-$ values in this study were similar to most mid- and low-latitude regions, but lower than those in polar regions ($\sim 32\text{‰}$). As listed in Table S1, the average $\Delta^{17}\text{O}-\text{NO}_3^-$ values in spring, summer, autumn, and winter were $28.8 \pm 8.0\text{‰}$, $25.5 \pm 2.20\text{‰}$, $25.6 \pm 1.35\text{‰}$, and $25.9 \pm 3.56\text{‰}$, respectively.

23. Lines 216–218: *Why was NO_2 formation not included in the discussion? It's central to $\Delta^{17}\text{O}(\text{NO}_3^-)$.*

Response: Thanks for your suggestion. We acknowledge that NO_2 formation plays a central role in controlling the $\Delta^{17}\text{O}-\text{NO}_3^-$. While direct measurements of NO_2 were not available during the campaign, we have addressed the $\text{NO}-\text{NO}_2$ conversion process indirectly through the parameter α , which represents the relative contribution of O_3 to

NO oxidation (Section 4.1). We acknowledge, however, that the absence of direct NO₂ observations introduces uncertainty, and we will consider the inclusion of NO₂ measurements in future field campaigns to better constrain this process. **(Line 326-333)**

Line 326-333: Typically, observations of $\Delta^{17}\text{O}-\text{NO}_3^-$ and estimated α (the proportion of O₃ oxidation in NO₂ production rate) values are employed to quantify the contributions of major NO₃⁻ oxidation pathway in conjunction with a Bayesian model. The α value ranged from 0.63 to 0.93, with an average of 0.83 ± 0.06 , suggesting the significance of O₃ participation in NO oxidation during the sampling campaign. On the other hand, our α values were lower than those (0.85-1) for other midlatitude regions (Alexander et al., 2009). The α values are influenced by the relative amount of O₃, HO₂ and RO₂ in NO_x cycling. Due to the generally high O₃ concentrations (O₃ > 50 ppb) observed in Lhasa, nearly all α values exceeded 0.8 (Figure S6).

24. Lines 220–223: Consider including a plot of this data.

Response: Thanks for your suggestion. We added it to the revised manuscript. **(Figure S5)/ (Line 307-308)**

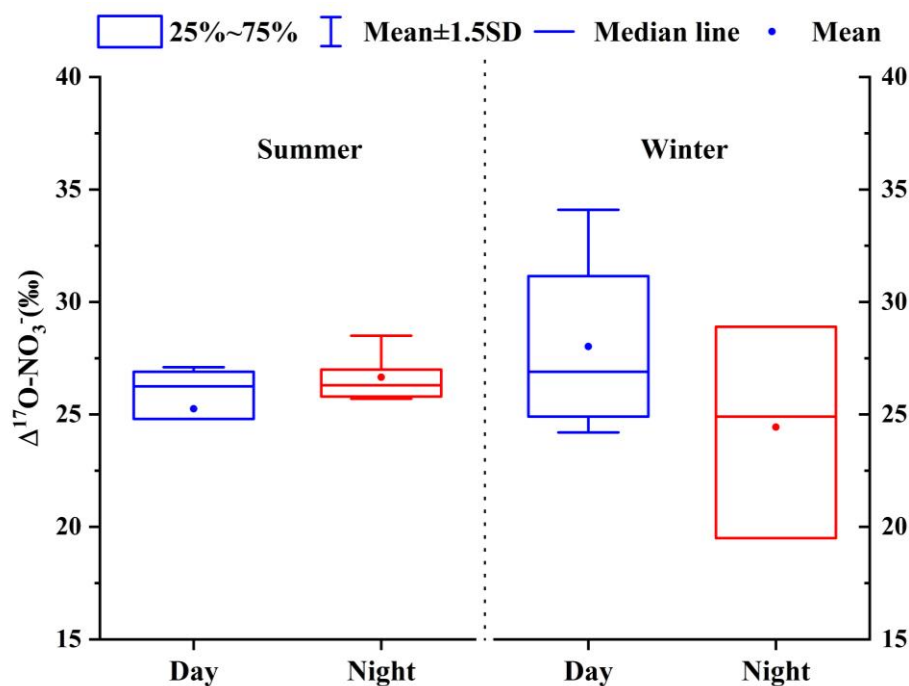


Figure S5 Diurnal variation of $\Delta^{17}\text{O}-\text{NO}_3^-$ values in summer and winter during the sampling campaign

Line 301-303: In contrast, the lower $\Delta^{17}\text{O-NO}_3^-$ values in other three seasons suggested a greater production of NO_3^- formation via $\text{NO}_2 + \text{OH}$ pathway, leading to more negative $\Delta^{17}\text{O-NO}_3^-$ values. Diurnal variation in $\Delta^{17}\text{O-NO}_3^-$ values also differed across season (Figure S5).

25. Lines 240–241: *A more detailed description of how α was determined is needed. A supplementary figure showing α and estimated $\Delta^{17}\text{O}(\text{NO}_2)$ over time would strengthen this section.*

Response: Thanks for your suggestion. A more detailed explanation of how the α value was determined has now been added in Section 2.4 of the revised manuscript. In particular, we clarified that α was estimated based on the relative contributions of O_3 , HO_2 , and RO_2 to NO_2 production, using their respective concentrations and reaction rate constants during the observation period.

To strengthen this section, we have included a new supplementary figure (Figure S6) presenting the time series of O_3 , HO_2 , RO_2 and α . Regarding $\Delta^{17}\text{O}(\text{NO}_2)$, we acknowledge that we were not able to directly measure $\Delta^{17}\text{O}$ in ozone ($\Delta^{17}\text{O-O}_3$) due to instrumental and logistical constraints. Instead, we adopted a literature-based value of $\Delta^{17}\text{O-O}_3^* = 39\text{‰}$. Because the $\Delta^{17}\text{O}$ in NO_2 is calculated via the equation ($\Delta^{17}\text{O-NO}_2 = \alpha \times \Delta^{17}\text{O-O}_3^*$), the temporal trend of estimated $\Delta^{17}\text{O-O}_3^*$ is similar to the α . We have added this explanation to the text. We also note that future work will aim to directly measure $\Delta^{17}\text{O-O}_3$ under high-altitude conditions like Lhasa to improve the estimation of $\Delta^{17}\text{O-NO}_2$. **(Line 321-328).**

Line 321-328: Typically, observations of $\Delta^{17}\text{O-NO}_3^-$ and estimated α (the proportion of O_3 oxidation in NO_2 production rate) values are employed to quantify the contributions of major NO_3^- oxidation pathway in conjunction with a Bayesian model. The α value ranged from 0.63 to 0.93, with an average of 0.83 ± 0.06 , suggesting the significance of O_3 participation in NO oxidation during the sampling campaign. On the other hand, our α values were lower than those (0.85-1) for other midlatitude regions (Alexander et al., 2009). The α values are influenced by the relative amount of O_3 , HO_2 and RO_2 in NO_x cycling. Due to the generally high O_3 concentrations ($\text{O}_3 > 50$ ppb) observed in

Lhasa, nearly all α values exceeded 0.8 (Figure S6).

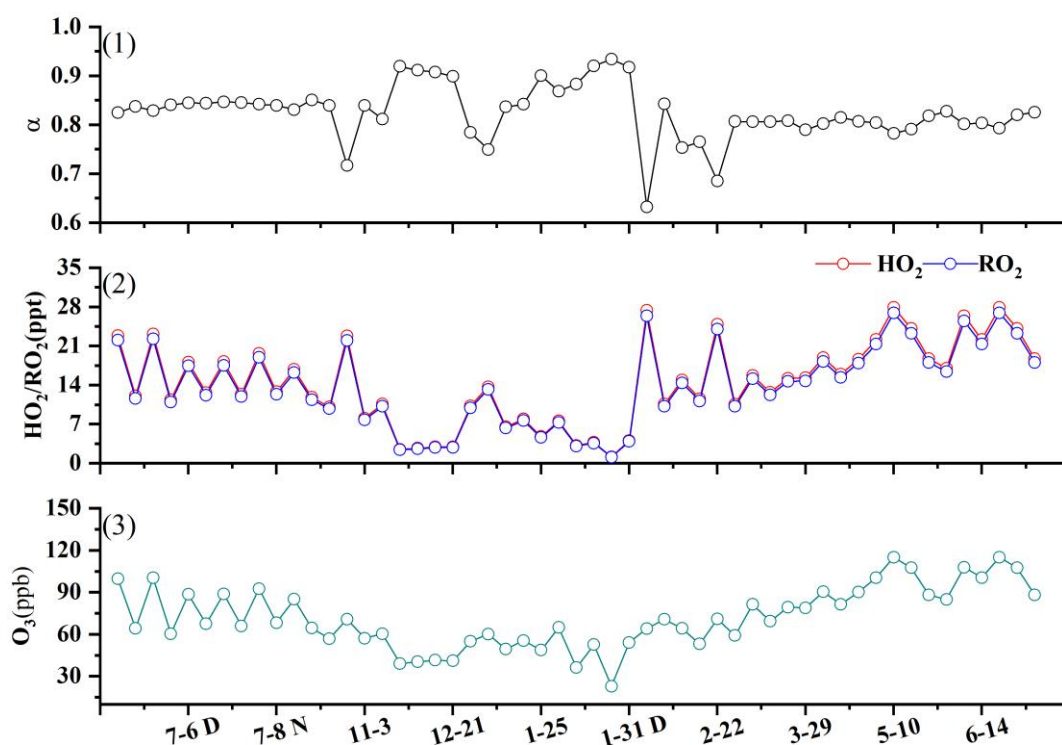


Figure S6 Time series of (1) α value; (2) HO_2 and RO_2 concentrations; (3) O_3 concentrations during the sampling campaign. The volume mixing ratios were calculated from mass concentrations ($\mu\text{g}/\text{m}^3$) based on the local atmospheric pressure and temperature conditions in Lhasa.

26. Lines 244–246: The pathway model lacks independent validation. Aside from the mixing model (which appears underconstrained), consider constructing a simple box model to test the plausibility of the proposed NO_3^- formation routes.

Response: Thanks for your thoughtful suggestion. We fully agree that independent validation using a mechanistic model, such as a box model, would help further test the plausibility of the proposed NO_3^- formation pathways. However, our current dataset is based on a year-long field observation, which is robust in terms of temporal coverage but lacks the necessary time-resolved gas-phase precursors (e.g., NO_3 , N_2O_5 , VOC) required to reliably constrain a box model. Therefore, we were unable to conduct an independent model validation at this stage. We acknowledge this as a limitation of the current study, and we have added a note (**4.4 Implication**) in the revised manuscript to highlight this point. In future work, we plan to incorporate box modeling and/or online measurements of key reactive species to better constrain the chemical mechanisms

involved.

27. Lines 252–253: *In most continental urban settings, $\text{NO}_3 + \text{VOC}$ is a minor contributor to aerosol nitrate. Reassess this conclusion in light of existing literature*

Response: Thank you for your suggestion. We acknowledge that in many continental urban environments, the $\text{NO}_3 + \text{VOC}$ pathway is typically considered a minor contributor to aerosol nitrate. However, Lhasa presents a distinct atmospheric setting, characterized by relatively high O_3 levels and significant VOC emissions from both local (e.g., biomass burning, incense burning, residential heating) and regional (e.g., long-range transport from South Asia) sources, especially during spring.

Growing evidence suggests that the southern Tibetan Plateau, including Lhasa, is impacted by long-range transported pollutants from South Asia in spring. As a result, it is likely that both locally emitted and transported VOC could participate in nocturnal NO_3 chemistry via the $\text{NO}_3 + \text{VOC}$ pathway. Nonetheless, we acknowledge the need for further observational and modelling studies to more quantitatively assess the importance of this pathway under high-altitude and complex emission conditions.

28. Lines 254–256: *If VOC data are available, use them to estimate the contribution of the $\text{NO}_3 + \text{VOC}$ pathway. Also, at this elevation, stratospheric intrusions may occur. Could this be a source of high $\Delta^{17}\text{O}$ nitrate?*

Response: Thanks for your insightful comment.

(1) Regarding the use of VOC data to estimate the contribution of the $\text{NO}_3 + \text{VOC}$ pathway:

Unfortunately, VOC concentrations were not simultaneously measured during our sampling campaign. Although Tang et al. (2022) reported that elevated VOC levels in Lhasa, the available VOC data had limited temporal resolution and lacked comprehensive speciation. As a result, it was not feasible to quantitatively constrain the $\text{NO}_3 + \text{VOC}$ pathway using observational VOC data. Future work integrating VOC data into a kinetic box model or MCM framework will help improve constraints on this pathway.

(2) Regarding the potential influence of stratospheric intrusion on $\Delta^{17}\text{O}-\text{NO}_3^-$:

We acknowledge the possibility of stratospheric intrusions at high elevations, which may introduce ozone with elevated $\Delta^{17}\text{O}-\text{NO}_3^-$ values. Previous studies have reported stratospheric intrusion events at high-altitude sites such as Nepal (5079 m a.s.l.) and Qomolangma Station (4300 m a.s.l.) during spring and winter. Given Lhasa's elevation and geographic setting, similar events may occur and could contribute to the enhanced $\Delta^{17}\text{O}-\text{NO}_3^-$ values observed in spring. This possible influence of a mixed stratospheric-tropospheric O_3 has been noted as a factor in NO_3^- formation during this period. We have added it to the revised manuscript. **(Line 410-419)**

Line 410-419: A significant increase in the $f_{\text{NO}_3+\text{VOC}}$ values was observed in spring ($p < 0.05$). First, O_3 and NO_2 are precursors of NO_3 . In this work, the highest concentrations of O_3 were found in spring ($114.9 \pm 18.1 \mu\text{g}/\text{m}^3$), likely leading to elevated NO_3 concentrations. Additionally, the low temperature and reduced OH radical concentrations in spring facilitate the reaction of NO_2 and O_3 to synthesize NO_3 . This might be an appropriate reason for the $f_{\text{NO}_3+\text{VOC}}$ values in spring. High-altitude locations such as Nepal (5079 m a.s.l.) and Qomolangma Station (4300 m a.s.l.) have experienced stratospheric ozone intrusions, especially in spring and winter, as reported in previous studies (Zhang et al., 2025; Cristofanelli et al., 2010; Morin et al., 2007; Zhang et al., 2022; Lin et al., 2016; Yin et al., 2017; Wang et al., 2020b). Notably, such intrusions in spring may elevate tropospheric O_3 levels in Lhasa, resulting in a mixture of tropospheric and stratospheric O_3 that enhances NO_3^- production.

29. Lines 283–284: *The logic in this sentence doesn't follow clearly from the preceding text. Please revise.*

Response: Thank you for pointing this out. We have revised the sentence to improve the logical flow. **(Line 398-403)**

Line 393-402: Figure S7 illustrates the seasonal variations in the relative contributions of the three main oxidation pathways to NO_3^- formation. When comparing different seasons, the $f_{\text{NO}_2+\text{OH}}$ values were lower ($p < 0.01$) in spring (22.6%) than in winter (50.8%), summer (52.9%) and autumn (73.2%). The dominance of $\text{NO}_2 + \text{OH}$ pathway in autumn is consistent with observations at Mt. Everest during the autumn seasons of

2017 and 2018, suggesting that NO_3^- formation on the Tibetan Plateau in autumn may be mainly driven by $\text{NO}_2 + \text{OH}$ pathway (Lin et al., 2021; Wang et al., 2020b).

30. Lines 286–287: High O_3 levels increase $\Delta^{17}\text{O}(\text{NO}_2)$, which strongly influences $\Delta^{17}\text{O}(\text{NO}_3^-)$. This should be acknowledged explicitly.

Response: Thank you for the insightful comment. We agree that high O_3 levels can elevate $\Delta^{17}\text{O}(\text{NO}_2)$, which in turn strongly affects $\Delta^{17}\text{O}(\text{NO}_3^-)$. Although we did not directly measure $\Delta^{17}\text{O}$ of NO_2 in this study, we evaluated the impact of O_3 on $\Delta^{17}\text{O}(\text{NO}_3^-)$ through the parameter α , which reflects the relative importance of NO_2 oxidation pathways involving O_3 . In Section 4.1 of the revised manuscript, we have explicitly discussed the influence of elevated O_3 concentrations on the α value in Lhasa.

31. Lines 295–297: Why is VOC assumed to be the only contribution from the biomass burning plume? Could oxidized nitrogen compounds also be transported?

Response: Thanks for your insightful comment. In our manuscript, VOC was considered a major contributor from the biomass burning primarily due to two reasons. First, previous studies have shown that VOC concentrations in Lhasa are comparable to those in the North China Plain, suggesting a relatively high local VOC level (e.g., Li et al., 2020). Second, our results indicate that the relative contribution of the $\text{NO}_3 + \text{VOC}$ pathway is significantly elevated in spring, a season when long-range transport from South Asia is active. Previous studies have reported that VOC originating from biomass burning and industrial emissions in South Asia can be transported to the Tibetan Plateau, leading to increased VOC concentrations. We therefore infer that the enhanced $f_{\text{NO}_3+\text{VOC}}$ in spring is largely driven by elevated VOC levels from both local and transported sources.

Nonetheless, we agree with the reviewer that oxidized nitrogen species (e.g., NO_x) are also present in biomass burning and may be co-transported to the region. These reactive nitrogen compounds could further participate in NO_3^- formation and cannot be ruled out as contributors. We have added clarification in the revised manuscript. **(Line 410-440)**

Line 410-440: A significant increase in the $f_{\text{NO}_3+\text{VOC}}$ values was observed in spring ($p < 0.05$). First, O_3 and NO_2 are precursors of NO_3 . In this work, the highest concentrations of O_3 were found in spring ($114.9 \pm 18.1 \mu\text{g}/\text{m}^3$), likely leading to elevated NO_3 concentrations. Additionally, the low temperature and reduced OH radical concentrations in spring facilitate the reaction of NO_2 and O_3 to synthesize NO_3 . This might be an appropriate reason for the $f_{\text{NO}_3+\text{VOC}}$ values in spring. High-altitude locations such as Nepal (5079 m a.s.l.) and Qomolangma Station (4300 m a.s.l.) have experienced stratospheric ozone intrusions, especially in spring and winter, as reported in previous studies (Zhang et al., 2025; Cristofanelli et al., 2010; Morin et al., 2007; Zhang et al., 2022; Lin et al., 2016; Yin et al., 2017; Wang et al., 2020b). Notably, such intrusions in spring may elevate tropospheric O_3 levels in Lhasa, resulting in a mixture of tropospheric and stratospheric O_3 that enhances NO_3^- production. Second, previous study has indicated that the Afghanistan-Pakistan-Tajikistan region, the Indo-Gangetic Plain, and Meghalaya-Myanmar region could transport industrial VOC to various zones in Tibet from west to east. Additionally, agricultural areas in northern India could contribute biomass burning-related VOC to the middle-northern and eastern regions of Tibet (Li et al., 2017). During our sampling campaign, South and Southeast Asia air clusters were notably prevalent in the springtime, coinciding with intensive fire spots observed in Afghanistan, Pakistan, India, Nepal, and Bhutan (Figure S3/S4). These observations, combined with the prevailing South and Southeast Asia air mass trajectories in spring, strongly suggest that long-range transported VOC from South Asia were delivered to Lhasa and likely participated in local NO_3^- production via $\text{NO}_3 + \text{VOC}$ pathway. Moreover, recent studies have shown that ambient VOC concentrations in the urban areas on the Qinghai-Tibet Plateau were comparable to those in the North China Plain (Tang et al., 2022). The input of VOC through long-range transport might further elevate VOC concentrations, thereby promoting NO_3^- formation via $\text{NO}_3 + \text{VOC}$ pathway and contributing to the enhanced $f_{\text{NO}_3+\text{VOC}}$ values observed in spring. While VOC appears to play a dominant role in the process, it should be noted that other nitrogen species (e.g., NO , NO_2) associated with biomass burning emissions may also be transported over long distances and influence NO_3^- formation in

Lhasa. These co-transported nitrogen compounds, although not directly quantified in this study, could further contribute to NO_3^- production in spring. Taken together, these findings provide strong evidence that long-range transport of biomass burning emissions, particularly from South Asia, can substantially influence springtime NO_3^- formation in Lhasa.

32. Lines 315–320: The diurnal nitrate interpretation doesn't account for the atmospheric lifetime of NO_3^- . Some residual NO_3^- from nighttime may persist into the daytime. Please consider this in the discussion.

Response: Thanks for your comment. In the revised manuscript, we have explicitly acknowledged the importance of the atmospheric lifetime of NO_3^- when interpreting diurnal variations in $\Delta^{17}\text{O}-\text{NO}_3^-$. **(Line 480-484)**

Line 480-484: Moreover, when interpreting the diurnal differences in $\Delta^{17}\text{O}-\text{NO}_3^-$ values, the atmospheric lifetime of NO_3^- must be considered. Given the atmospheric lifetime of NO_3^- is generally more than 12 hours, each sample might reflect both daytime and nighttime NO_3^- production impacting on $\Delta^{17}\text{O}-\text{NO}_3^-$ values (Park et al., 2004; Vicars et al., 2013).

33. Lines 319–320: NO_3 and N_2O_5 chemistry is unlikely to significantly contribute to daytime NO_3^- formation due to their short lifetimes in sunlight. Please calculate and discuss the expected lifetime.

Response: Thanks for your comment. We fully agree that NO_3 and N_2O_5 radicals are highly reactive species with short atmospheric lifetimes under sunlight. Due to the limited availability of concurrent photolysis rate data and relevant concentrations (NO_3 and N_2O_5 concentrations) during our sampling campaign, we were unable to quantitatively calculate the daytime atmospheric lifetimes of these species at our site. Nevertheless, we have revised the manuscript to include a more explicit discussion based on previous studies. **(Line 450-484)**

Line 450-484: Interestingly, distinct diurnal patterns of NO_3^- oxidation pathways were observed during the sampling campaign (Figure 5). In summer, $\text{NO}_2 + \text{OH}$ pathway

showed a significantly higher contribution during the daytime (55.1%) compared to nighttime ($44.9\pm\%$), which is attributed to increased OH radical synthesis during longer days and higher temperatures in Lhasa (Rohrer and Berresheim, 2006). A previous study indicated that lower NO_2 and higher O_3 concentrations enhance the relative contribution of OH pathway to NO_3^- formation (Wang et al., 2019). Additionally, the concentration of ALWC (the detailed information is given in Text S3) was higher at night than during the day in summer, favoring NO_3^- formation through nocturnal formation. In winter, $f_{\text{NO}_2+\text{OH}}$, $f_{\text{NO}_3+\text{VOC}}$ and $f_{\text{N}_2\text{O}_5+\text{H}_2\text{O}}$ were similar during both day and night. Typically, photolytic destruction and chemical reactions with NO are rapid sinks during the daytime, with lifetimes generally less than 5 seconds and resulting in extremely low concentrations. Similarly, the atmospheric lifetime of N_2O_5 under sunlight is also very short (Wang et al., 2018). Thus, daytime NO_3 and N_2O_5 chemistry is often considered negligible. However, a recent study revealed that a non-negligible amount of NO_3 radicals can persist during the daytime in cold months, owing to the limited solar radiation (Hellén et al., 2018). Wang et al. (2020a) found that the daytime production rate of NO_3 can be substantial due to elevated concentrations of O_3 and NO_2 , suggesting that the mixing ratios of NO_3 and N_2O_5 during the day may not be negligible. Furthermore, in winter, lower temperatures and elevated NO_2 concentrations facilitate a quasi-steady-state equilibrium between NO_3 and N_2O_5 , slowing the overall reactivity of the NO_3^- precursors (Brown et al., 2003). This equilibrium condition minimizes diurnal fluctuations in precursor concentrations, resulting in relatively stable nocturnal and daytime NO_3^- formation pathways, including $\text{NO}_3 + \text{VOC}$ and $\text{N}_2\text{O}_5 + \text{H}_2\text{O}$. Nevertheless, we acknowledge that the exact role of daytime $\text{NO}_3/\text{N}_2\text{O}_5$ chemistry remains uncertain in Lhasa and should be further assessed using concurrent field observations or chemical transport models. Moreover, when interpreting the diurnal differences in $\Delta^{17}\text{O}-\text{NO}_3^-$ values, the atmospheric lifetime of NO_3^- must be considered. Given the atmospheric lifetime of NO_3^- is generally more than 12 hours, each sample might reflect both daytime and nighttime NO_3^- production impacting on $\Delta^{17}\text{O}-\text{NO}_3^-$ values (Park et al., 2004; Vicars et al., 2013).

35. Figure 5: Uncertainty/error bars are needed for all pathway contributions. These are model-derived estimates with inherent uncertainties and should not be presented as precise values.

Response: Thanks for your suggestion. We agree that the pathway contributions are model-derived estimates and should be presented with appropriate uncertainties. In the revised manuscript, we have added error bars to represent the uncertainties associated with each pathway contribution.

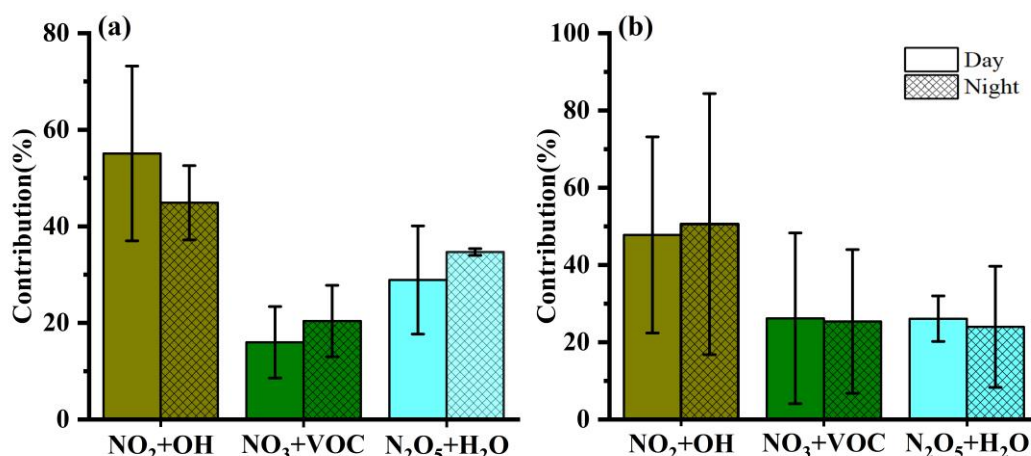


Figure 5. the relative contributions (mean \pm SD values) of $\text{NO}_2 + \text{OH}$, $\text{NO}_3 + \text{VOC}$, and $\text{N}_2\text{O}_5 + \text{H}_2\text{O}$ to NO_3^- formation during the day and night (a) in summer and (b) winter in Lhasa during the sampling campaign.

36. Lines 355–364: Much of the mechanistic discussion here is speculative. Consider using a simple model framework (e.g., kinetic or box model) to evaluate the chemical feasibility of the proposed pathways.

Response: Thanks for your suggestion. We fully agree that incorporating a simple model framework such as a box or kinetic model would provide stronger mechanistic support for evaluating the chemical feasibility of the proposed pathways. However, due to the current lack of sufficient observational data (e.g., VOC, radical concentrations), we are unable to implement such a model in the present study. We acknowledge this limitation in the revised manuscript and will prioritize the development of a modelling component in our future work to improve the mechanistic understanding of NO_3^- formation under high-altitude conditions.

Reference

- Alexander, B., Hastings, M., Allman, D., Dachs, J., Thornton, J., and Kunasek, S.: Quantifying atmospheric nitrate formation pathways based on a global model of the oxygen isotopic composition ($\Delta^{17}\text{O}$) of atmospheric nitrate, *Atmospheric Chemistry and Physics*, 9, 5043-5056, 2009.
- Brown, S. S., Stark, H., and Ravishankara, A.: Applicability of the steady state approximation to the interpretation of atmospheric observations of NO_3 and N_2O_5 , *Journal of Geophysical Research: Atmospheres*, 108, 2003.
- Cao, X., Xing, Q., Hu, S., Xu, W., Xie, R., Xian, A., Xie, W., Yang, Z., and Wu, X.: Characterization, reactivity, source apportionment, and potential source areas of ambient volatile organic compounds in a typical tropical city, *Journal of Environmental Sciences*, 123, 417-429, 2023.
- Cristofanelli, P., Bracci, A., Sprenger, M., Marinoni, A., Bonafè, U., Calzolari, F., Duchi, R., Laj, P., Pichon, J.-M., and Roccato, F.: Tropospheric ozone variations at the Nepal Climate Observatory-Pyramid (Himalayas, 5079 m asl) and influence of deep stratospheric intrusion events, *Atmospheric Chemistry and Physics*, 10, 6537-6549, 2010.
- Daily, B., <https://xinwen.bjd.com.cn/content/s6340d130e4b0b60bbc5d4ecd.html>
- Fan, M.-Y., Zhang, Y.-L., Lin, Y.-C., Hong, Y., Zhao, Z.-Y., Xie, F., Du, W., Cao, F., Sun, Y., and Fu, P.: Important role of NO_3 radical to nitrate formation aloft in urban Beijing: Insights from triple oxygen isotopes measured at the tower, *Environmental Science & Technology*, 56, 6870-6879, 2021.
- Feng, X., Chen, Y., Chen, S., Peng, Y., Liu, Z., Jiang, M., Feng, Y., Wang, L., Li, L., and Chen, J.: Dominant Contribution of NO_3 Radical to NO_3^- Formation during Heavy Haze Episodes: Insights from High-Time Resolution of Dual Isotopes $\Delta^{17}\text{O}$ and $\delta^{18}\text{O}$, *Environmental Science & Technology*, 57, 20726-20735, 2023.
- He, S., Huang, M., Zheng, L., Chang, M., Chen, W., Xie, Q., and Wang, X.: Seasonal variation of transport pathways and potential source areas at high inorganic nitrogen wet deposition sites in southern China, *Journal of Environmental Sciences*, 114, 444-453, <https://doi.org/10.1016/j.jes.2021.12.024>, 2022.

- Hellén, H., Praplan, A. P., Tykkä, T., Ylivinkka, I., Vakkari, V., Bäck, J., Petäjä, T., Kulmala, M., and Hakola, H.: Long-term measurements of volatile organic compounds highlight the importance of sesquiterpenes for the atmospheric chemistry of a boreal forest, *Atmospheric Chemistry and Physics*, 18, 13839-13863, 2018.
- Ishino, S., Hattori, S., Savarino, J., Jourdain, B., Preunkert, S., Legrand, M., Caillon, N., Barbero, A., Kuribayashi, K., and Yoshida, N.: Seasonal variations of triple oxygen isotopic compositions of atmospheric sulfate, nitrate, and ozone at Dumont d'Urville, coastal Antarctica, *Atmospheric Chemistry and Physics*, 17, 3713-3727, 2017.
- Kanaya, Y., Cao, R., Akimoto, H., Fukuda, M., Komazaki, Y., Yokouchi, Y., Koike, M., Tanimoto, H., Takegawa, N., and Kondo, Y.: Urban photochemistry in central Tokyo: 1. Observed and modeled OH and HO₂ radical concentrations during the winter and summer of 2004, *Journal of Geophysical Research: Atmospheres*, 112, 2007.
- Kunasek, S., Alexander, B., Steig, E., Hastings, M., Gleason, D., and Jarvis, J.: Measurements and modeling of $\Delta^{17}\text{O}$ of nitrate in snowpits from Summit, Greenland, *Journal of Geophysical Research: Atmospheres*, 113, 2008.
- Lhasa, T. P. s. G. o., Overview of Lhasa: <https://www.lasa.gov.cn/lasa/yxls/yx.shtml>
- Li, H., He, Q., Song, Q., Chen, L., Song, Y., Wang, Y., Lin, K., Xu, Z., and Shao, M.: Diagnosing Tibetan pollutant sources via volatile organic compound observations, *Atmospheric Environment*, 166, 244-254, 2017.
- Li, Z., Walters, W. W., Hastings, M. G., Song, L., Huang, S., Zhu, F., Liu, D., Shi, G., Li, Y., and Fang, Y.: Atmospheric nitrate formation pathways in urban and rural atmosphere of Northeast China: Implications for complicated anthropogenic effects, *Environmental Pollution*, 296, 118752, <https://doi.org/10.1016/j.envpol.2021.118752>, 2022.
- Lin, M., Zhang, Z., Su, L., Hill-Falkenthal, J., Priyadarshi, A., Zhang, Q., Zhang, G., Kang, S., Chan, C. Y., and Thiemens, M. H.: Resolving the impact of stratosphere-to-troposphere transport on the sulfur cycle and surface ozone over the Tibetan Plateau using a cosmogenic ³⁵S tracer, *Journal of Geophysical Research: Atmospheres*, 121, 439-456, 2016.

- Lin, Y.-C., Zhang, Y.-L., Yu, M., Fan, M.-Y., Xie, F., Zhang, W.-Q., Wu, G., Cong, Z., and Michalski, G.: Formation mechanisms and source apportionments of airborne nitrate aerosols at a Himalayan-Tibetan Plateau site: Insights from nitrogen and oxygen isotopic compositions, *Environmental Science & Technology*, 55, 12261-12271, 2021.
- Michalski, G., Scott, Z., Kabling, M., and Thiemens, M. H.: First measurements and modeling of $\Delta^{17}\text{O}$ in atmospheric nitrate, *Geophysical Research Letters*, 30, 2003.
- Morin, S., Savarino, J., Bekki, S., Gong, S., and Bottenheim, J.: Signature of Arctic surface ozone depletion events in the isotope anomaly ($\Delta^{17}\text{O}$) of atmospheric nitrate, *Atmospheric Chemistry and Physics*, 7, 1451-1469, 2007.
- Park, R. J., Jacob, D. J., Field, B. D., Yantosca, R. M., and Chin, M.: Natural and transboundary pollution influences on sulfate-nitrate-ammonium aerosols in the United States: Implications for policy, *Journal of Geophysical Research: Atmospheres*, 109, 2004.
- Rohrer, F. and Berresheim, H.: Strong correlation between levels of tropospheric hydroxyl radicals and solar ultraviolet radiation, *Nature*, 442, 184-187, 2006.
- Savarino, J., Vicars, W. C., Legrand, M., Preunkert, S., Jourdain, B., Frey, M. M., Kukui, A., Caillon, N., and Gil Roca, J.: Oxygen isotope mass balance of atmospheric nitrate at Dome C, East Antarctica, during the OPALE campaign, *Atmospheric Chemistry and Physics*, 16, 2659-2673, 2016.
- Tang, G., Yao, D., Kang, Y., Liu, Y., Liu, Y., Wang, Y., Bai, Z., Sun, J., Cong, Z., Xin, J., Liu, Z., Zhu, Z., Geng, Y., Wang, L., Li, T., Li, X., Bian, J., and Wang, Y.: The urgent need to control volatile organic compound pollution over the Qinghai-Tibet Plateau, *iScience*, 25, 105688, <https://doi.org/10.1016/j.isci.2022.105688>, 2022.
- Vicars, W., Morin, S., Savarino, J., Wagner, N., Erbland, J., Vince, E., Martins, J., Lerner, B., Quinn, P., and Coffman, D.: Spatial and diurnal variability in reactive nitrogen oxide chemistry as reflected in the isotopic composition of atmospheric nitrate: Results from the CalNex 2010 field study, *Journal of Geophysical Research: Atmospheres*, 118, 50567-50588, 2013.
- Vicars, W. C. and Savarino, J.: Quantitative constraints on the ^{17}O -excess ($\Delta^{17}\text{O}$)

- signature of surface ozone: Ambient measurements from 50 N to 50 S using the nitrite-coated filter technique, *Geochimica et Cosmochimica Acta*, 135, 270-287, 2014.
- Vicars, W. C., Bhattacharya, S., Erbland, J., and Savarino, J.: Measurement of the ^{17}O -excess ($\Delta^{17}\text{O}$) of tropospheric ozone using a nitrite-coated filter, *Rapid Communications in Mass Spectrometry*, 26, 1219-1231, 2012.
- Wang, H., Chen, X., Lu, K., Hu, R., Li, Z., Wang, H., Ma, X., Yang, X., Chen, S., Dong, H., Liu, Y., Fang, X., Zeng, L., Hu, M., and Zhang, Y.: NO_3 and N_2O_5 chemistry at a suburban site during the EXPLORE-YRD campaign in 2018, *Atmospheric Environment*, 224, 117180, <https://doi.org/10.1016/j.atmosenv.2019.117180>, 2020a.
- Wang, H., Lu, K., Guo, S., Wu, Z., Shang, D., Tan, Z., Wang, Y., Le Breton, M., Lou, S., Tang, M., Wu, Y., Zhu, W., Zheng, J., Zeng, L., Hallquist, M., Hu, M., and Zhang, Y.: Efficient N_2O_5 uptake and NO_3 oxidation in the outflow of urban Beijing, *Atmos. Chem. Phys.*, 18, 9705-9721, 10.5194/acp-18-9705-2018, 2018.
- Wang, K., Hattori, S., Kang, S., Lin, M., and Yoshida, N.: Isotopic constraints on the formation pathways and sources of atmospheric nitrate in the Mt. Everest region, *Environmental Pollution*, 267, 115274, 2020b.
- Wang, Y. L., Song, W., Yang, W., Sun, X. C., Tong, Y. D., Wang, X. M., Liu, C. Q., Bai, Z. P., and Liu, X. Y.: Influences of atmospheric pollution on the contributions of major oxidation pathways to $\text{PM}_{2.5}$ nitrate formation in Beijing, *Journal of Geophysical Research: Atmospheres*, 124, 4174-4185, 2019.
- Yin, X., Kang, S., de Foy, B., Cong, Z., Luo, J., Zhang, L., Ma, Y., Zhang, G., Rupakheti, D., and Zhang, Q.: Surface ozone at Nam Co in the inland Tibetan Plateau: variation, synthesis comparison and regional representativeness, *Atmospheric Chemistry and Physics*, 17, 11293-11311, 2017.
- Zhang, Y.-L., Zhang, W., Fan, M.-Y., Li, J., Fang, H., Cao, F., Lin, Y.-C., Wilkins, B. P., Liu, X., and Bao, M.: A diurnal story of $\Delta^{17}\text{O}(\text{NO}_3^-)$ in urban Nanjing and its implication for nitrate aerosol formation, *npj Climate and Atmospheric Science*, 5, 50, 2022.
- Zhang, Y., Zhao, T., Ning, G., Xu, X., Chen, Z., Jia, M., Sun, X., Shu, Z., Lu, Z., and

Liu, J.: A unique mechanism of ozone surges jointly triggered by deep stratospheric intrusions and the Tibetan Plateau topographic forcing, *Geophysical Research Letters*, 52, e2024GL114207, 2025.

Zhao, M., Huang, Z., Qiao, T., Zhang, Y., Xiu, G., and Yu, J.: Chemical characterization, the transport pathways and potential sources of PM_{2.5} in Shanghai: Seasonal variations, *Atmospheric Research*, 158, 66-78, 2015.